

This is the author's final, peer-reviewed manuscript as accepted for publication (AAM). The version presented here may differ from the published version, or version of record, available through the publisher's website. This version does not track changes, errata, or withdrawals on the publisher's site.

## X-ray induced radiation damage in CLYC(Ce)

S. Richards and G.J. Sykora

### Published version information

**Citation:** S Richards and G Sykora. "X-ray induced radiation damage in CLYC(Ce)." Nuclear Instruments and Methods in Physics Research Section A, vol. 902 (2018): 45-50.

**DOI:** [10.1016/j.nima.2018.06.045](https://doi.org/10.1016/j.nima.2018.06.045)

©2018. This manuscript version is made available under the [CC-BY-NC-ND](https://creativecommons.org/licenses/by-nc-nd/4.0/) 4.0 Licence.

This version is made available in accordance with publisher policies. Please cite only the published version using the reference above. This is the citation assigned by the publisher at the time of issuing the AAM. Please check the publisher's website for any updates.

This item was retrieved from **ePubs**, the Open Access archive of the Science and Technology Facilities Council, UK. Please contact [epubs@stfc.ac.uk](mailto:epubs@stfc.ac.uk) or go to <http://epubs.stfc.ac.uk/> for further information and policies.

# Accepted Manuscript

X-ray induced radiation damage in CLYC(Ce)

S. Richards, G.J. Sykora

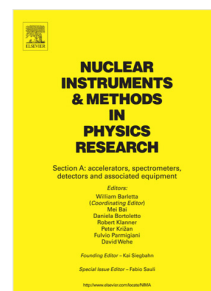
PII: S0168-9002(18)30766-6  
DOI: <https://doi.org/10.1016/j.nima.2018.06.045>  
Reference: NIMA 60906

To appear in: *Nuclear Inst. and Methods in Physics Research, A*

Received date: 22 March 2018  
Revised date: 29 May 2018  
Accepted date: 14 June 2018

Please cite this article as: S. Richards, G.J. Sykora, X-ray induced radiation damage in CLYC(Ce), *Nuclear Inst. and Methods in Physics Research, A* (2018), <https://doi.org/10.1016/j.nima.2018.06.045>

This is a PDF file of an unedited manuscript that has been accepted for publication. As a service to our customers we are providing this early version of the manuscript. The manuscript will undergo copyediting, typesetting, and review of the resulting proof before it is published in its final form. Please note that during the production process errors may be discovered which could affect the content, and all legal disclaimers that apply to the journal pertain.



# X-ray Induced Radiation Damage in CLYC(Ce)

S. Richards<sup>1\*</sup> & G. J. Sykora<sup>2</sup>

[1] Detector Development Group – Science and Technology Facilities Council, Rutherford Appleton Laboratory, Harwell Science and Innovation Campus, Didcot, Oxfordshire, OX11 0QX. These authors contributed equally to this work. [2] ISIS Detector Group – Science and Technology Facilities Council, Rutherford Appleton Laboratory, Harwell Science and Innovation Campus, Didcot, Oxfordshire, OX11 0QX

\*Corresponding Author: sion.richards@stfc.ac.uk

## Abstract

The radiation hardness of the <sup>6</sup>Li loaded scintillator CLYC(Ce) to X-rays was investigated. Two crystals were studied; one crystal was irradiated with X-rays and one was kept as a control and only exposed to a moderated <sup>241</sup>Am-Be source. The control crystal was used as a reference sample for photoluminescence excitation and emission measurements. The exposed crystal was given two doses of X-rays, the first was 2.3 Gy and the second was 118.2 Gy after a 22 week annealing period. The total dose was 120.5 Gy and was found to significantly reduce the light yield of the crystal. Pulse height spectra from the moderated <sup>241</sup>Am-Be taken with the irradiated crystal showed a 54% decrease in pulse height and a broadening of the FWHM of the peak from 14.6 % to 44.2%. Analysis of the pulse shapes showed no change to the median decay time to 37% of the scintillator, with values of ~350 ns for the irradiated and control crystal. Photoluminescence excitation and emission measurements revealed a reduction in the relative intensity of the main Ce<sup>3+</sup> emission with respect to the self-trapped exciton luminescence. This indicated a modification to the Ce<sup>3+</sup> luminescence center. There was little recovery at room temperature over the course of 22 weeks after the first irradiation. The irradiated crystal was also found to display significant room temperature luminescence after X-ray irradiation with it being measurable up to 120 minutes after the X-ray irradiation.

Keywords: Scintillator; Radiation Damage; Thermal Neutron Detection; Pulse shape discrimination; Afterglow

## 1. Introduction

New and upgraded neutron scattering facilities such as the European Spallation Source in Sweden [1], J-PARC in Japan [2], the Spallation Neutron Source in the United States [3] and the ISIS pulsed neutron and muon source in the United Kingdom [4] produce high neutron fluxes for materials science. ISIS is a neutron spallation source which is used to generate thermal and epithermal neutrons and muons. There are currently 30 neutron scattering instruments in ISIS which are dedicated to applications including neutron reflectometry, powder and single crystal diffraction, small angle scattering and imaging. Neutron sensitive scintillators such as ZnS:Ag/<sup>6</sup>LiF and <sup>6</sup>Li-glass are currently used on ISIS [5]. These scintillators have disadvantages like long afterglow for ZnS:Ag/<sup>6</sup>LiF and high sensitivity for the <sup>6</sup>Li-glass [4]. Because of these disadvantages, new neutron sensitive scintillators are regularly evaluated to determine their suitability for use at ISIS.

Due to inaccessibility and cost restrictions in neutron scattering instrumentation, instruments are expected to have a lifetime of ~20 years. Radiation hard detectors are therefore required. High neutron fluxes also give rise to high backgrounds of  $\gamma$ -rays. Therefore, damage from both of these

40 sources of radiation must be evaluated. The group of van Eijk at the Delft University of Technology  
41 have performed a thorough, though non-exhaustive, development and characterization of thermal  
42 neutron scintillators for multiple applications including spallation neutron sources [6-8].

43 One of the promising neutron sensitive scintillators is Cerium activated  $\text{Cs}_2\text{LiYCl}_6$  (CLYC(Ce))  
44 isotopically enriched with  $^6\text{Li}$ . CLYC(Ce) is typically used for dual mode  $\gamma$ -ray and neutron detection  
45 where the  $^6\text{Li}$  is used for thermal neutrons and the  $^{35}\text{Cl}(n,p)^{35}\text{S}$  reaction allows for fast neutron  
46 detection. CLYC(Ce) has been shown to have energy resolution in the order of 4-5%, a 1  $\mu\text{s}$  decay  
47 time allowing for operation at rates in the order of 100's of kcps, and excellent pulse shape  
48 discrimination (PSD) properties [9-13]. PSD arises from the complex decay characteristics of  
49 scintillation light in CLYC(Ce) where a  $\gamma$ -ray will induce 3 ns core-valence luminescence in addition to  
50 the typical 50 ns and 1000 ns decay components while a neutron event will scintillate with a greater  
51 probability of the slower 1000 ns decay. This difference of decay enables PSD, allowing for clear  
52 discrimination between neutron events and  $\gamma$ -ray events. The different scintillation mechanisms  
53 observed in CLYC(Ce) that gives rise to PSD have been thoroughly studied with substantial data on  
54 the decay characteristics and emission wavelengths available [11, 12, 15].

55 The authors could only find 2 published studies on the radiation hardness of CLYC(Ce). Both studies  
56 focused on the suitability to CLYC(Ce) for space radiation environments and using proton beams to  
57 characterize radiation hardness. Both studies found that proton irradiation induced the formation of  
58 color centers in CLYC(Ce) resulting in a reduction of performance [12,13].

59 This work presents measurements on X-ray induced changes to the luminescent properties of  
60 commercially purchased CLYC(Ce). Suitability of CLYC(Ce) for use in instruments at neutron science  
61 facilities where long term stability under significant neutron and  $\gamma$ -ray exposures is assessed.

## 62 **2. Method**

63 Two 2.54 cm diameter 5 mm thick CLYC(Ce) crystals canned in aluminum with a white reflector and  
64 quartz windows were purchased from the same supplier from the same batch so they would be of  
65 similar quality. The irradiated crystal was denoted Crystal 1 and the control was denoted Crystal 2.  
66 The components of the study were; X-ray irradiations, neutron measurements and luminescence  
67 measurements. The crystals were stored in a dark, temperature controlled, dry nitrogen cabinet  
68 between irradiations and measurements to investigate room temperature annealing and to ensure  
69 there was no optical stimulation of any filled traps.

### 70 **2.1 X-ray irradiations**

71 Two sets of X-ray irradiations were performed using tungsten anode X-ray sets. The dose was  
72 measured using a Radcal Accu-Gold + with the Radcal 10x6-6 ionization chamber. The first  
73 irradiation was to a dose of 2.3 Gy at 160 kVp, 50  $\mu\text{A}$  for 45 minutes at a source to crystal distance of  
74 10 cm. Crystal 1 was then given a second X-ray irradiation after a 22 week annealing period. This  
75 second and final irradiation was to a dose of 118.2 Gy delivered over 10 minutes at 60 kVp 50 mA  
76 with a source to crystal distance of 33.5 cm.

### 77 **2.2 Neutron Measurements**

78 The neutron detection performance was measured using a paraffin moderated  $^{241}\text{Am-Be}$  source by  
79 monitoring the pulse height of the  $^6\text{Li}$  neutron capture peak as a function dose and by evaluating the  
80 pulse shape discrimination performance. For these measurements the crystals were mounted on a  
81 ETL 9902 PMT biased at -900 V with index matching optical grease the signal was integrated for 50  
82 ns and read out by an Acqiris 400 MSps 14-bit digitizer. Pulse shape discrimination was performed by  
83 measuring the time for each digitized pulse to reach 37% of its peak amplitude. The neutron  
84 detection performance of Crystal 1 was measured after both X-ray irradiations and at 12 weeks into  
85 the 22 week annealing period between X-ray irradiations.

### 86 **2.3 Luminescence Measurements**

87 Both radio- and photoluminescence measurements were performed to study any changes to the  
88 luminescent properties of the crystals as a function of dose. The radioluminescence spectrum was  
89 acquired using an Ocean Optics USB2000+UV-VIS spectrometer with a fiber coupled f1.0 fused silica  
90 lens. It was only measured for Crystal 1 during the first X-ray irradiation in a light tight X-ray set.  
91 These measurements were completed within the first 5 minutes of the 45 minute X-ray irradiation  
92 which equated to a dose of 0.25 Gy.

93 Excitation and emission photoluminescence maps were acquired using a Horiba FluoroMax-4  
94 Spectrofluorometer. The excitation and emission photoluminescence maps were acquired after 12  
95 weeks into the 22 week annealing period, and two maps of Crystal 1 were measured following the  
96 2<sup>nd</sup> irradiation, the first was 2 hours after the final irradiation and the second was 24 hours after the  
97 final irradiation. Crystal 2 was also measured for comparison. A long lived room temperature  
98 luminescence or afterglow was measured in Crystal 1 immediately following the 2<sup>nd</sup> irradiation, this  
99 was achieved blocking out the excitation source of the spectrofluorometer and was measured 10, 30  
100 and 120 minutes after the irradiation.

101

102

## **3. Results**

103 Both CLYC(Ce) crystals showed the presence of several macro defects in the crystals which included  
104 cracks and voids. The volume around the macro defects in crystal 1 developed a blue discoloration  
105 after only 2.3 Gy of X-ray irradiation (Fig. 1 top). The bulk of Crystal 1 also developed the same blue  
106 discoloration after 120.5 Gy (Fig. 1 bottom).

107



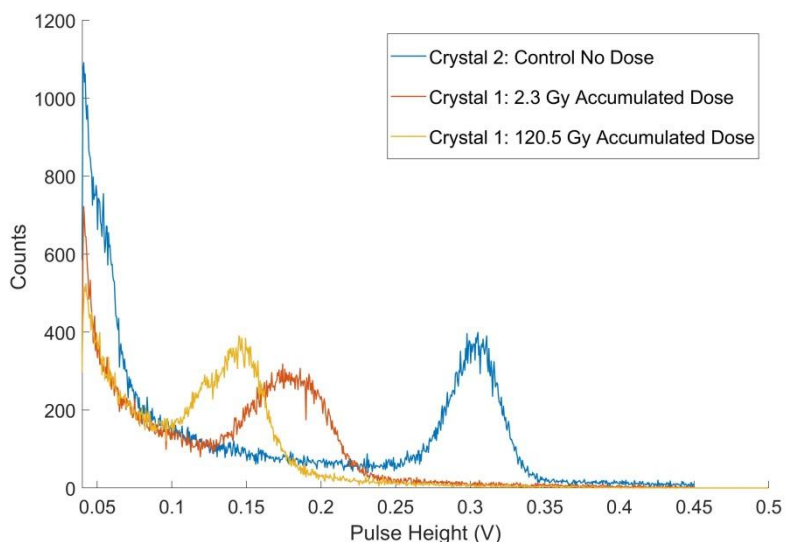
108

109 Figure 1. A photograph of both Commercially bought CLYC(Ce)crystals after the 1<sup>st</sup> irradiation (top)  
110 and the 2nd irradiation (bottom), note the discoloration and the macro-defects.

111

### 3.1 Neutron Measurements

112 Pulse height spectra of the crystals exposed to neutrons and  $\gamma$ -ray from the moderated  $^{241}\text{Am-Be}$   
113 after every irradiation are shown in figure 2. The FWHM of the  $^6\text{Li}$  neutron capture peak of Crystal 1  
114 was significantly broader after irradiation of 2.3 Gy than the control, Crystal 2 (Fig. 2). The FWHM of  
115 Crystal 2's  $^6\text{Li}$  peak was 14.6% compared to Crystal 1's 40.5% after 2.3 Gy and 44.2% after the  
116 irradiation of 118.2 Gy or accumulated dose of 120.5 Gy (Table 1). The pulse height of the neutron  
117 capture peak also decreased with X-ray irradiation. The peak reduced from 0.3 mV for the control, to  
118 0.175 mV after the first irradiation and 0.138 mV after the final irradiation.

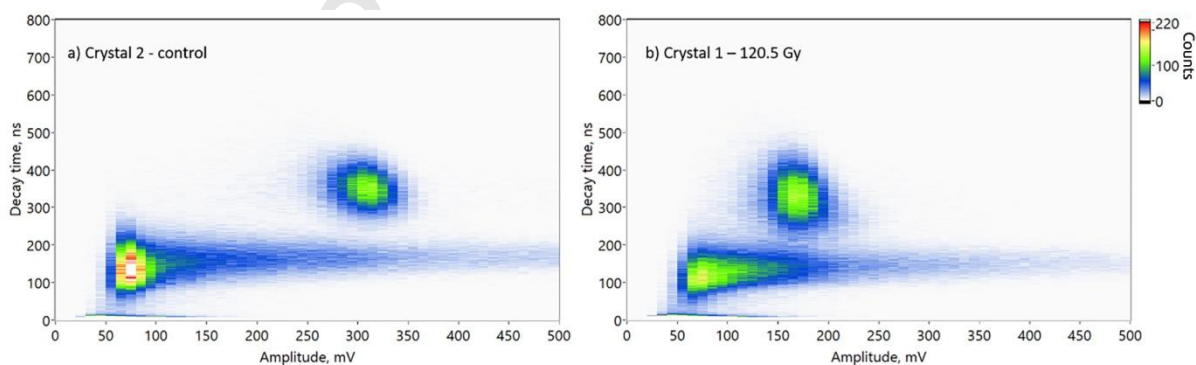


119

120 Figure 2. Pulse Height Spectra of the CLYC(Ce) crystals, showing the control crystal and the irradiated  
 121 crystal after both sets of X-ray irradiation

122

123 Figure 3 shows 2D histograms of decay time (defined here as the time it takes for the signal to  
 124 reduce to 37% of the peak amplitude) versus pulse height for each event in both Crystal 1 after  
 125 120.5 Gy and Crystal 2. The median decay time for both crystals was found to be  $\sim 350$  ns for the  
 126 neutron events and did not change with irradiation. The broadening in Crystal 1 after 120.5 Gy is  
 127 attributed to the reduced pulse height. The ratio of  $\gamma$ -ray events in the region from around 75 mV to  
 128 150 mV also appear to change. This is a consequence of the lower energy Compton scatter events  
 129 being lost because of the reduction in the crystal's light output. The pulse height is shown to reduce  
 130 for both  $\gamma$ -ray and neutron capture events as in the pulse height spectra shown in Figure 2. This  
 131 reduction in light output by a factor of  $\sim 2$  in Crystal 1 results in a broadening of the decay time  
 132 profile of the Compton scattered events. The decay time profile is broadened by a similar factor for  
 133 both the  $\gamma$ -ray events and thermal neutron events at the same pulse height.



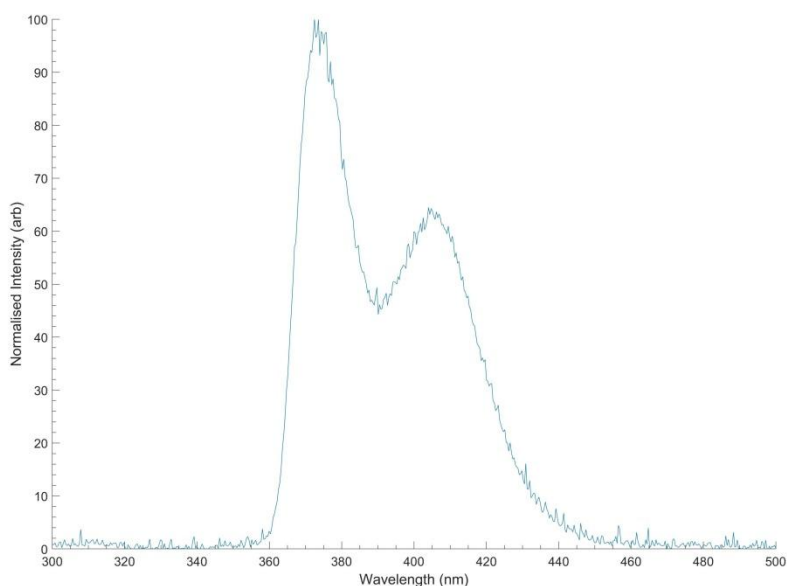
134

135 Figure 3. Pulse shape discrimination plots of Crystal 2 (left) and Crystal 1 after exposure to 120.5 Gy  
 136 of X-ray irradiation.

137

### 3.2 Radioluminescence Measurements

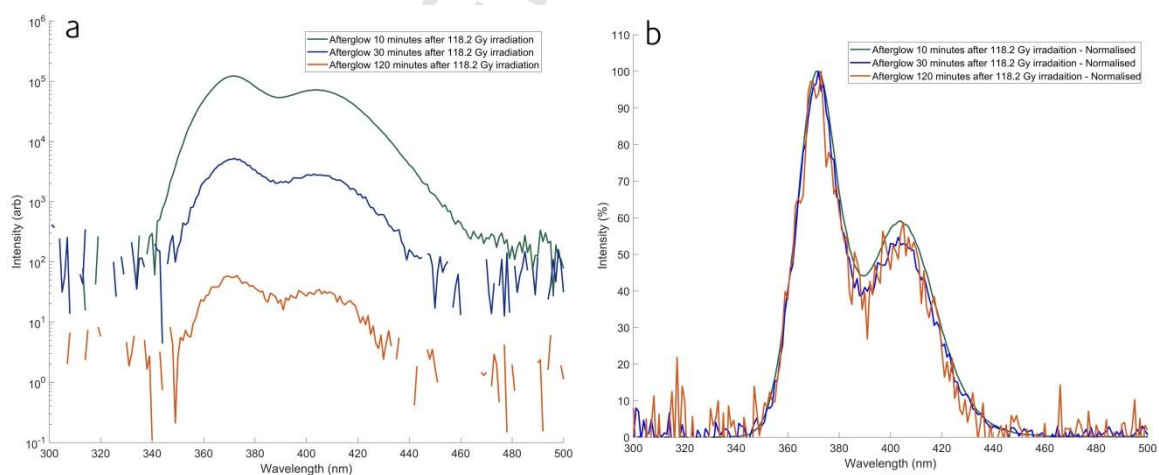
138 The radioluminescence spectrum of Crystal 1 did not show any changes to the emission during  
 139 irradiation (Fig. 4), however the dose delivered to the crystal was only 0.25 Gy. The emission peaks  
 140 were found to be at 372 nm and 405 nm with a ratio of 5:3 and match reported values in the  
 141 literature for the  $\text{Ce}^{3+}$  emission [9-11, 14, 15].



142

143 Figure 4. The radioluminescence spectrum of the CLYC(Ce) Crystal 1 prior to irradiation damage.

144 After the 2<sup>nd</sup> irradiation of 118.2 Gy, Crystal 1 was found to have developed room temperature  
 145 luminescence or afterglow which was visible by eye and was still measureable 120 minutes after X-  
 146 ray irradiation (Fig. 5(a)). The afterglow had the same emission spectrum as the radioluminescence  
 147 spectrum with peaks at 372 nm and 405 nm along with the same 5:3 peak ratio (Fig. 4 and 5 (b)).



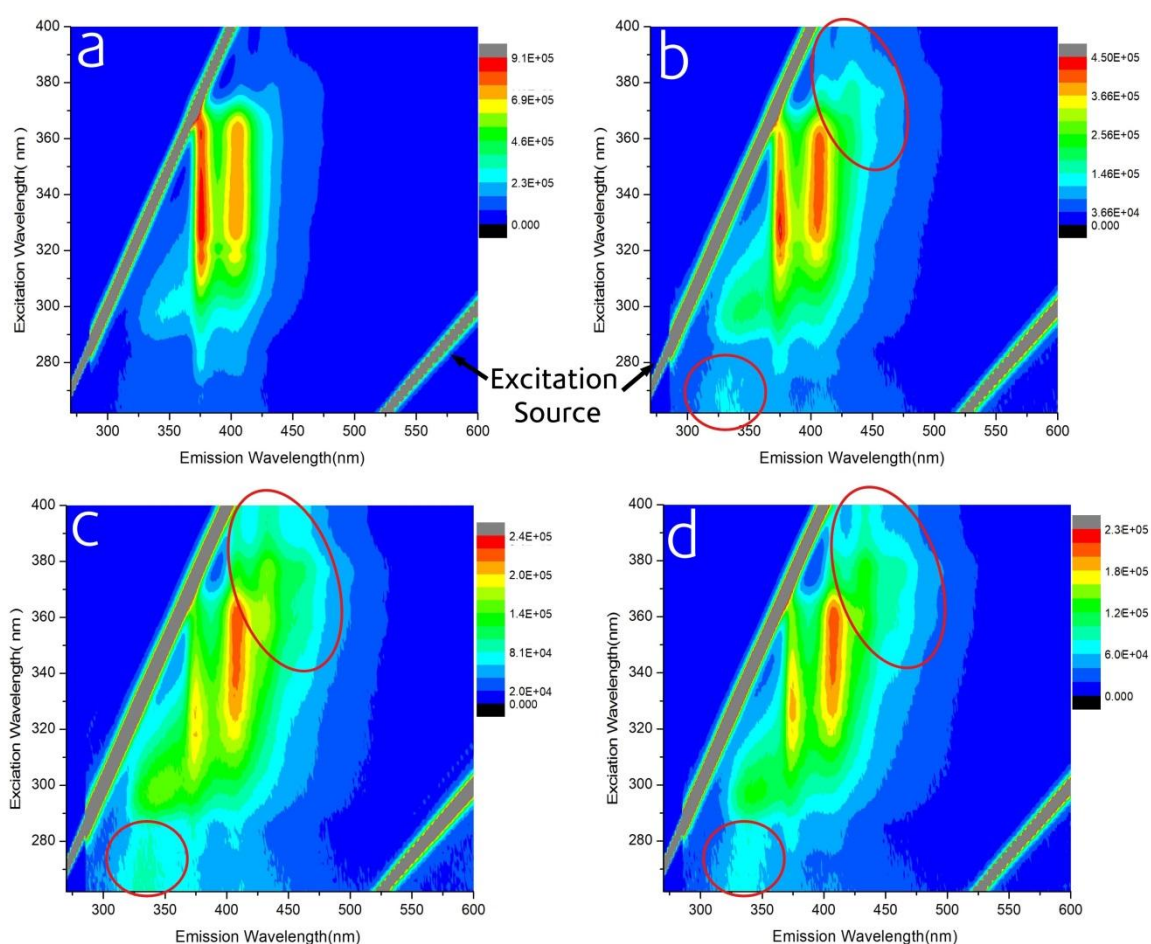
148

149 Figure 5. Luminescence spectra of the Afterglow from the X-ray irradiated CLYC(Ce) crystal 10  
 150 minutes, 30 minutes and 120 minutes after irradiation with 118.2 Gy. a) Directly comparable  
 151 intensity on a logarithmic axis and b) intensity normalized to the 372 nm peak.

152

### 3.3 Photoluminescence Measurements

153 The photoluminescence spectrum of Crystal 2 was found to be similar to Crystal 1's  
 154 radioluminescence spectrum prior to radiation damage. The only difference being the peak ratios,  
 155 which was 5:3 for the radioluminescence and 5:4 for the photoluminescence. However, after  
 156 irradiation the photoluminescence spectrum of Crystal 1 was found to differ significantly from  
 157 Crystal 2 (Fig. 6). The ratio between the 375 nm and 405 nm emissions had changed to 10:9 as  
 158 opposed to 5:4 in Crystal 2 (Table 1). The relative intensity of the main  $\text{Ce}^{3+}$  emission lines to other  
 159 minor emissions changed significantly. The reduction in the intensity of the  $\text{Ce}^{3+}$  emission resulted in  
 160 the 340 nm emission, excited by 270 nm light becoming significantly more prominent (circled red in  
 161 Fig 6. B-D). This reduction in intensity also resulted in the 325 nm and 450 nm emissions being more  
 162 prominent, effectively broadening the appearance of the main  $\text{Ce}^{3+}$  emission. The second irradiation  
 163 of 118.2 Gy caused a further reduction in the intensity of the  $\text{Ce}^{3+}$  emission with respect to the 340,  
 164 325 and 450 nm emissions. It also caused the 370 nm emission in Crystal 1 to be less intense than  
 165 the 405 nm peak (Fig. 6 c) with a change in the peak ratio from 5:4 to 10:11. Repeating the  
 166 photoluminescence map after 24 hours showed that there was some recovery in the relative  
 167 intensity of these minor peaks to the  $\text{Ce}^{3+}$  emission. The 370 nm peak and the 405 nm peak also  
 168 showed some recovery to a ratio of 21:20. Table 1 summarizes the results obtained from all of the  
 169 measurements described above.



170

171 Figure 6. Excitation-Emission photoluminescence maps of Crystal 2 (a), Crystal 1 after the first  
 172 irradiation of 2.3 Gy (b), 120 minutes after the 2<sup>nd</sup> irradiation of 118.2 Gy (c), and 24 hours after the

173 2<sup>nd</sup> irradiation of 118.2 Gy (d). The regions circled in red become more prominent with X-ray dose.  
 174 The diagonal lines are the first and second order diffraction lines from the excitation source.

175

176

177

178 Table 1: A summary of measured performance parameters for the tested CLYC(Ce) crystals

Sample	<sup>6</sup> Li Peak Height	<sup>6</sup> Li decay time to 37%	FWHM	Ratio of 375 nm to 405 nm photoluminescence emission (330nm excitation)
Crystal 2 (Control)	0.3 mV	355 ns	14.6%	5:4
Crystal 1 (2.3 Gy dose)	0.175 mV	356 ns	40.5%	10:9
Crystal 1 (120.5 Gy dose) 2 hours after irradiation	Not measured	353 ns	Not Measured	10:11
Crystal 1 (120.5 Gy dose) 24 hours after irradiation	0.138 mV	354 ns	44.2%	21:20

179

180

181

#### 4. Discussion

182 The commercially purchased CLYC(Ce) crystal showed low tolerance for X-ray irradiation with a dose  
 183 of 2.3 Gy inducing significant changes to the luminescence properties. The  $\gamma$ -ray dose exposed to the  
 184 instruments at ISIS is not accurately measured because of the technical challenges it poses.

185 However, off-axis  $\gamma$ -ray monitors placed near the T0 chopper report a dose rate of 0.5 mSv/hour.

186 This is expected to give an underestimate of the dose an instrument would receive resulting in a  
 187 lifetime of about 4000 hours or less for these CLYC(Ce) crystals. It should be noted that the crystals  
 188 were purchased in 2015 when CLYC(Ce) was new to the market and developments in the crystal  
 189 growth could have increased the radiation hardness of these crystals.

190

191 Radiation damage in scintillators is a complicated topic with a variety of possible radiation damage  
 192 mechanisms ranging from the introduction of absorption bands, changes in the scintillation process  
 193 and/or radiation induced chemical reactions [14]. The initial X-ray radioluminescence spectrum of  
 194 Crystal 1 before it was heavily irradiated matched the photoluminescence spectrum of Crystal 2,  
 195 except for a difference in ratio between the 375 nm and 405 nm emission peaks (Table 1). The  
 196 measured afterglow of Crystal 1 after the 118.2 Gy irradiation also shared the same Ce<sup>3+</sup> emission  
 197 peaks and ratio of those peaks as the radioluminescence spectrum. While Crystal 1 did become  
 198 discolored after the irradiation, it can be concluded from the afterglow spectrum that there was no

199 self-absorption of the  $Ce^{3+}$  emission. The PSD plots show that the decay time to 37% is unaffected by  
200 the X-ray irradiation. This leads to the conclusion that the primary scintillation process is still present  
201 with no new processes being created. The afterglow would not alter the decay time on the PSD plots  
202 as it's much lower than the 37% intensity threshold used. The reduction in the intensity of the  $Ce^{3+}$   
203 emission with respect to the other emission lines suggests a formation of a non-radiative  
204 recombination pathway. This pathway could be caused by the transformation of the  $Ce^{3+}$  to  $Ce^{4+}$   
205 which is known to quench  $Ce^{3+}$  luminescence [14]. The other peaks which became more prominent  
206 with radiation damage have been attributed to STE luminescence [15]. This STE luminescence would  
207 not be affected by any radiation induced changes to the oxidation state of the cerium in the crystal.  
208 Therefore it is plausible that the  $Ce^{3+}$  in the irradiated crystal is being modified by the X-ray  
209 irradiation, causing a reduction in light yield. This however does not explain the cause of the very  
210 long lived room temperature luminescence. Formation of shallow traps is a possible mechanism of  
211 the long lived afterglow which would also support a reduction in scintillation pulse height. Further  
212 work to resolve these unanswered questions is needed involving thermoluminescence  
213 measurements and techniques such as EPR to probe the valence state of cerium but is beyond the  
214 scope of this work.

## 215 5. Conclusion

216 The radiation hardness of CLYC(Ce) to X-ray irradiation was tested using two commercially  
217 purchased CLYC(Ce) crystals. One crystal was irradiated and the other was kept as a control.  
218 Significant radiation damage was observed after an X-ray dose of 2.3 Gy with only small amounts of  
219 recovery at room temperature. A subsequent dose of 118.2 Gy was found to induce further changes  
220 in the scintillation properties of the crystal. Radiation damage caused a reduction in pulse height of  
221 the  ${}^6Li$  neutron capture peak of CLYC(Ce) but the primary decay time remained unchanged. The  ${}^6Li$   
222 neutron capture peak showed a 54 % reduction in pulse height when compared to the control crystal  
223 and broadening of the FWHM of the peak from 14.6 % to 44.2%. Analysis of the luminescent  
224 properties of the crystal showed that the irradiated crystal had a long lived room temperature  
225 luminescence or afterglow and the photoluminescence measurements showed significant changes  
226 to the emission spectrum of the crystal. Further analysis would be required to fully understand these  
227 changes and to which could potentially increase the radiation hardness of CLYC(Ce) to X-ray  
228 radiation. The associated degradation in the neutron detection performance of the crystal means  
229 that, at the present time, they are not suitable for use at facilities such as ISIS due to the  
230 requirement to operate for long periods of time in high  $\gamma$ -ray dose environments.

## 231 Acknowledgments

232 This work was funded by the Science and Technology Facilities Council (STFC) through the ISIS department and  
233 the Centre for Instrumentation (CFI). We would also like to thank Matt Wilson and Paul Sellar of the STFC's  
234 Technology Department's Detector Development Group and Nigel Rhodes and Erik Schooneveld of STFC's ISIS  
235 Neutron Detector Group for supporting this work.

## 237 References

238 [1] I. Stefanescu, M. Christensen, J. Fenske, R. Hall-Wilton, P. Henry, O. Kirstein, M. Muller, G.  
239 Nowak, D. Pooley, D. Raspino, N. Rhodes, J. Saroun, J. Schefer, E. Schooneveld, J. Sykora and W.

- 240 Schweika, "Neutron detectors for the ESS diffractometers," *Journal of Instrumentation*, vol. 12, p.  
241 01019, 2017.
- 242 [2] J-PARC Materials and Life Science Facility [online]. Available: [https://j-](https://j-parc.jp/MatLife/en/index.html#)  
243 [parc.jp/MatLife/en/index.html#](https://j-parc.jp/MatLife/en/index.html#), [accessed March 2018].
- 244 [4] Spallation Neutron Source [online]. Available: <https://neutrons.ornl.gov/sns>, [accessed March  
245 2018].
- 246 [4] N. J. Rhodes, E. M. Schooneveld and R. S. Eccleston, Current status and future directions of  
247 position sensitive neutron detectors at ISIS, *Nucl. Instrum. Meth. A*, vol. 529, pp. 243-248, 2004.
- 248 [5] G. J. Sykora, E. M. Schooneveld and N. J. Rhodes, ZnO:Zn/<sup>6</sup>LiF scintillator – A low afterglow  
249 alternative to ZnS:Ag/<sup>6</sup>LiF for thermal neutron detection, *Nucl. Instrum. Meth. A*, vol. 883, pp. 75-82,  
250 2018.
- 251 [6] C. W. E. van Eijk, Neutron PSDs for the next generation of spallation neutron sources, *Nucl.*  
252 *Instrum. Meth. A*, vol. 477, pp. 383-390, 2002.
- 253 [7] C. W. E. van Eijk, A. Bessière, P. Dorenbos, Inorganic thermal-neutron scintillators, *Nucl. Instrum.*  
254 *Meth. A*, vol. 529, pp. 260-267, 2004.
- 255 [8] C. W. E. van Eijk, Inorganic Scintillators for Thermal Neutron Detection, *Trans. Nucl. Sci.*, vol. 59,  
256 pp. 2242-2247, 2012.
- 257 [9] Whitney, C., Stapels, C., Johnson, E., Chapman, E., Alberghini, G., Glodo, J., Shah, K., Christian, J.  
258 (2011). 6-Li enriched Cs<sub>2</sub>LiYCl<sub>6</sub>:Ce Based Thermal Neutron Detector Coupled with CMOS Solid-State  
259 Photomultipliers for a Portable Detector Unit. *Proceedings of SPIE*, 7961(1), 79610U–79610U–6.  
260 <https://doi.org/10.1117/12.878225>
- 261 [10] Whitney, C. M., Chen, X. J., Johnson, E., Staples, C. J., Chapman, E., Alberghini, G., Rines, R., Van  
262 Loef, E., Glodo, J., Shah, K., Christian, J. F. (2011). Radiation Effects on a Potential Scintillation-Based  
263 Solid-State Spectrometer Prototype for Compact Monitoring of Space Radiation/Weather Satellite  
264 Conditions. *IEEE Transactions on Nuclear Science*, 58(6), 3095–3102.  
265 <https://doi.org/10.1109/TNS.2011.2172955>
- 266 [11] Glodo, J., Hawrami, R., & Shah, K. S. (2013). Development of Cs<sub>2</sub>LiYCl<sub>6</sub> scintillator. *Journal of*  
267 *Crystal Growth*, 379, 73–78. <https://doi.org/10.1016/j.jcrysgro.2013.03.023>
- 268 [12] D'Olympia, N., Chowdhury, P., Lister, C. J., Glodo, J., Hawrami, R., Shah, K., & Shirwadkar, U.  
269 (2013). Pulse-shape analysis of CLYC for thermal neutrons, fast neutrons, and gamma-rays. *Nuclear*  
270 *Instruments and Methods in Physics Research Section A: Accelerators, Spectrometers, Detectors and*  
271 *Associated Equipment*, 714, 121–127. <https://doi.org/10.1016/j.nima.2013.02.043>
- 272 [13] Mesick, K. E., Coupland, D. D. S., Nowicki, S. F., & Stonehill, L. C. (2017). The Effects of Radiation  
273 Damage on CLYC Performance, 273–280. <https://arxiv.org/abs/1711.11170>
- 274 [14] Lecoq, P., Gektin, A., & Korzhik, M. (2017). *Inorganic Scintillators for Detector Systems*. Cham:  
275 Springer International Publishing. <https://doi.org/10.1007/978-3-319-45522-8>
- 276 [15] Van Loef, E. V.D., Dorenbos, P., Van Eijk, C. W. E., Krämer, K. W., & Güdel, H. U. (2002).  
277 Scintillation and spectroscopy of the pure and Ce<sup>3+</sup>-doped elpasolites: Cs<sub>2</sub>LiYX<sub>6</sub> (X = Cl, Br). *Journal*  
278 *of Physics Condensed Matter*, 14(36), 8481–8496. <https://doi.org/10.1088/0953-8984/14/36/307>